

## Publication P9

Sami Ruoho, Jere Kolehmainen, Jouni Ikäheimo, and Antero Arkkio. 2010. Interdependence of demagnetization, loading, and temperature rise in a permanent-magnet synchronous motor. IEEE Transactions on Magnetics, volume 46, number 3, pages 949-953.

© 2010 Institute of Electrical and Electronics Engineers (IEEE)

Reprinted, with permission, from IEEE.

This material is posted here with permission of the IEEE. Such permission of the IEEE does not in any way imply IEEE endorsement of any of Aalto University's products or services. Internal or personal use of this material is permitted. However, permission to reprint/republish this material for advertising or promotional purposes or for creating new collective works for resale or redistribution must be obtained from the IEEE by writing to [pubs-permissions@ieee.org](mailto:pubs-permissions@ieee.org).

By choosing to view this document, you agree to all provisions of the copyright laws protecting it.

# Interdependence of Demagnetization, Loading, and Temperature Rise in a Permanent-Magnet Synchronous Motor

Sami Ruoho<sup>1,2</sup>, Jere Kolehmainen<sup>3</sup>, Jouni Ikäheimo<sup>3</sup>, and Antero Arkkio<sup>1</sup>

<sup>1</sup>Department of Electrical Engineering, Helsinki University of Technology, Espoo FI-02015, Finland

<sup>2</sup>Neorem Magnets Oy, Ulvila, FIN-28400 Finland

<sup>3</sup>ABB Oy, Motors, Vaasa FI-65101, Finland

The demagnetization of permanent magnets in permanent-magnet machines has been under discussion in many publications lately. Demagnetization models have been used, for example, to optimize the machine structures but there have been no studies on how the demagnetization is coupled with the loading and temperature-rise of the machine and how this coupling should be modeled. In this paper, we model the dynamics of the demagnetization of a dovetail machine under a constant load torque. We show that the thermal model should be included in the demagnetization calculations. The demagnetization will cause an increase of the copper losses, which will increase the temperatures of the machine. This will cause more demagnetization and might lead even to a stall in a situation in which a model neglecting the thermal effects predicts stable operation without additional demagnetization.

*Index Terms*—Demagnetization, dovetail machine, finite-element analysis, permanent magnets, synchronous machines.

## I. INTRODUCTION

THE demagnetization of the permanent magnets in permanent-magnet machines has been discussed in many publications recently. The demagnetization has been modeled either by linear models [1], [2], hysteresis models [3], [4] or by models based on single valued non-linear demagnetisation curves [5]. Both parametric [6] and finite-element models [3], [7] have been used to study the machine operation under the risk of demagnetization. The effect of the partial demagnetization on the shape of EMF has been studied [1], [8]. Some authors have studied, how the demagnetization has been divided inside a single magnet [9], [10]. Different motor types have been compared [10] and optimized [7] against demagnetization. Even motors using several magnet grades have been developed using these models [11], [12]. Diagnostics has also been studied to detect demagnetization [13]. The demagnetization phenomenon itself has mostly been ignored. No comprehensive study has been made of the interdependence of demagnetization, loading and temperature-rise in a PM machine and how these effects should be modeled to get relevant results.

When a machine loaded with a constant torque is demagnetized partially, it will start to draw more current to produce the required torque. The increased current may cause more demagnetization, which will again increase the current (Fig. 1). The increased current will cause more copper losses, which will cause temperatures to rise, dropping the intrinsic coercivity of the permanent magnets and making them more prone to demagnetization. It is important to study, if this process keeps on going until the machine stalls. It is also important to study, how the point where the demagnetization stops could be most easily estimated.

In this paper, the dynamics of the demagnetization in permanent magnets of a synchronous machine is studied. The same demagnetization situation is modeled in different ways and the

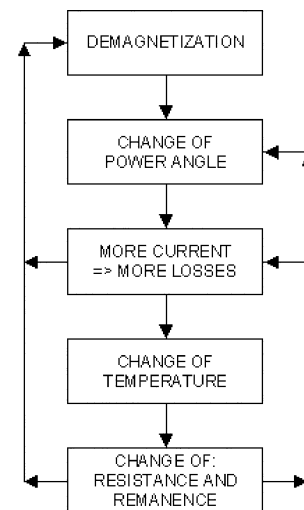


Fig. 1. A diagram representing the dynamics of demagnetization of the permanent magnets in an electrical machine loaded with a constant torque.

results are compared. The effects of the loading and thermal behavior of the machine on the demagnetization are studied. The effect of the shape of the hysteresis curve on the demagnetization is also modeled.

## II. MACHINE

A dovetail machine [14] is a special type of buried magnet machine where the mechanical loads caused by the rotation are carried by the magnets [15]. The mechanical properties of the dovetail machines are extensively studied by Kolehmainen *et al.* in [16] and [17]. The performance of the dovetail machine is compared to the performance of the other types of buried magnet machines in [18].

The machine modeled in this study is a 6-pole dovetail machine of 45 kW. The machine has sintered NdFeB magnets in three poles (Fig. 2), while the other poles without magnets act

Manuscript received June 24, 2009; revised August 29, 2009; accepted September 27, 2009. First published October 09, 2009; current version published February 18, 2010. Corresponding author: S. Ruoho (e-mail: sami.ruoho@neorem.fi).

Digital Object Identifier 10.1109/TMAG.2009.2033592

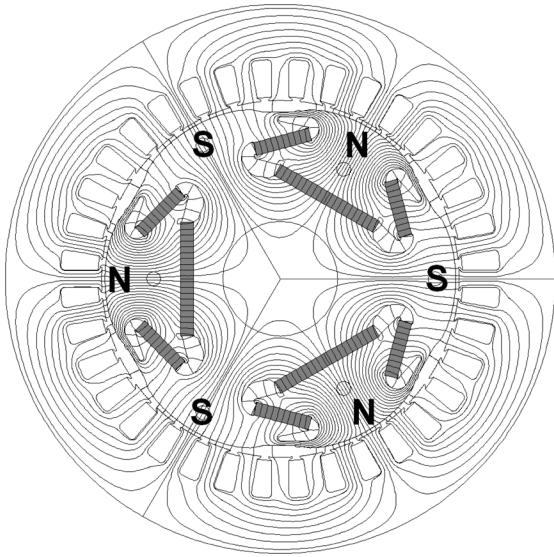


Fig. 2. A cut of a six-pole motor [12] used in the present study.

TABLE I  
MAIN PARAMETERS OF THE MODELED MACHINE [12]

Parameter:	Value
Number of poles	6
Outer diameter of the stator	310 mm
Air gap diameter	165 mm
Core length	165 mm
Number of stator slots	36
Connection	Delta
Input frequency	300 Hz
Rated speed	6000 rpm
Rated voltage (phase-to-phase)	370 V
Rated power	45 kW
Maximum power	67 kW
Magnet material	Sintered NdFeB
$B_r$ of PM material at 20 °C	1.15 T
$jH_c$ of PM material at 20 °C	-2100 kA/m
$B_r$ of PM material at 190 °C	0.90 T
$jH_c$ of PM material at 190 °C	-280 kA/m

$B_r$  denotes the remanence,  $jH_c$  the intrinsic coercivity of the magnet material

as a return path for the flux. The parameters of the machine are presented in Table I.

### III. MODEL

#### A. FEM Model

The calculations in this paper have been done using a special FEM software developed by Helsinki University of Technology. The program solves both the field equations and circuit equations simultaneously. The mathematics of the software is more thoroughly described in [19]. The calculations were done using the time-stepping method. The rotor was rotating at the same constant speed as the stator field in most calculations. In some calculations, a mechanical model was used, where the rotation speed was dependent on the torque developed by the machine and the moment of inertia. The mechanical model allowed the modeling of the oscillation of the power angle.

One third of the machine cross section was modeled with FEM. The second-order mesh contained 3234 elements and 7377 nodes. The magnets were modeled with 103 elements.

#### B. Demagnetization Model

A demagnetization model developed before [5] was implemented in the FEM software described above. The demagnetization model is thoroughly described in [5], [11], and [9]. The model takes into account the temperature dependence of the magnetic properties, the squareness of the hysteresis curve, and the direction of the demagnetizing field. The demagnetization model checks the demagnetization of each element inside permanent magnets after each time-step. If any demagnetization is detected, the magnetization of that element is adjusted and the time-step is recalculated.

Very often, the demagnetization models consider only the field component antiparallel to the magnetization direction, because it is assumed that the perpendicular component does not have any effect on demagnetization [20]. It is shown in [21] and [9] that the field component perpendicular to the magnetization direction must also be taken into account.

#### C. Temperature Model

The magnetic properties of sintered NdFeB magnets are highly dependent on temperature. Both the remanence and intrinsic coercivity decrease with the rising temperature [5]. The decreasing remanence will make the machine to draw more current, if it is loaded with a constant torque. The decreasing intrinsic coercivity makes the magnets more vulnerable on demagnetization. The copper losses are also temperature dependent, since the resistivity of copper changes a lot as a function of temperature. For these reasons, it is important to have a thermal model, which will give the temperatures of permanent magnets and windings in a machine as a function of the losses.

It is not important to involve the thermal calculations directly in the electromechanical calculations. The electric phenomena in an electric machine take place in a matter of several electric cycles. The time needed to change the temperatures in a large electric machine is a lot longer, because of the large heat capacity of the machine. This is why electric modeling and thermal modeling can be done using different models, which communicate by exchanging information using some simple parameters (Fig. 3). The losses of the machine are fed from the FEM model to the thermal model, which returns the temperatures of the machine to the FEM model. The remanence and the intrinsic coercivity of the magnets and the resistivity of the magnets and copper are temperature dependent.

The thermal model used in these calculations is a very simple network of thermal resistances (Fig. 4). The model is based on an assumption, that all losses generated by the machine ( $P_{Fe}$ ,  $P_{rotor}$ ,  $P_{Cu}$ ) are dissipated to the ambient (point of  $T_{Ambient}$ ) via stator iron (point of  $T_{Fe}$ ) through the thermal resistance  $R_{FA}$ . The rotor losses ( $P_{rotor}$ ) are transferred to stator over the air-gap thermal resistance ( $R_{RF}$ ). The copper losses ( $P_{Cu}$ ) are transferred to stator iron over the thermal resistance  $R_{CF}$ . Because the capacitances are missing, this simple model suits only for steady-state modeling.

The temperatures and the losses of the machine were measured and calculated in the past testing [12]. The thermal resis-

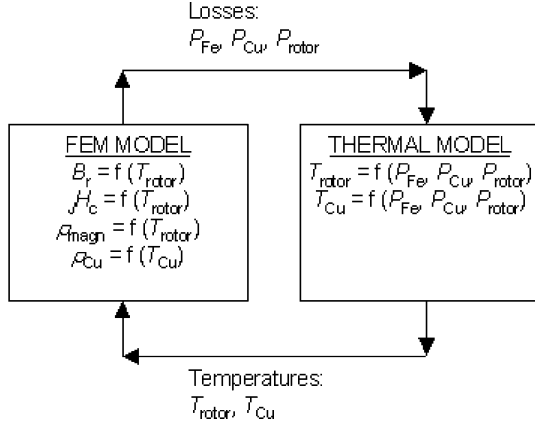


Fig. 3. The interface between the FEM model and the thermal model is handled by exchanging information of losses and temperatures. The temperatures will have an effect on remanence ( $B_r$ ), intrinsic coercivity ( $JH_c$ ) and resistivity of magnet material ( $\rho_{\text{magn}}$ ) and copper ( $\rho_{\text{Cu}}$ ).

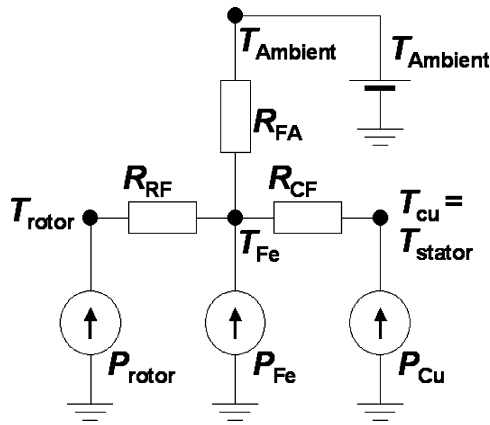


Fig. 4. Simple thermal model used in this study. The losses ( $P_{\text{rotor}}$ ,  $P_{\text{Fe}}$ ,  $P_{\text{Cu}}$ ) calculated by FEM software are inputs of the thermal model. The values of the rotor temperature  $T_{\text{rotor}}$  and winding temperature  $T_{\text{Cu}}$  are inserted to FEM software. The thermal resistances ( $R_{\text{RF}}$ ,  $R_{\text{CF}}$ ,  $R_{\text{FA}}$ ) are adjusted to model the real thermal behavior of the motor. The ambient temperature  $T_{\text{Ambient}}$  is increased to cause demagnetization in this study.

tances ( $R_{\text{RF}}$ ,  $R_{\text{CF}}$ ,  $R_{\text{FA}}$ ) of the model (Fig. 4) were estimated based on these results.

#### IV. SIMULATIONS

The purpose of this paper is to study how the demagnetization of a machine should be calculated to get accurate results. A machine loaded with a constant torque is modeled in several ways, which are described in the following subsections.

The calculation scenarios are selected to create a demagnetization of approximately  $-5\%$ . This level of demagnetization is still acceptable in many applications, because it is close to the manufacturing tolerance of the remanence of the magnets.

The demagnetizing situation is caused in these calculations by a high temperature, which is achieved by increasing the ambient temperature ( $T_{\text{Ambient}}$  in Fig. 4) of the motor loaded with the rated torque heavily. However, it is not possible to separate the contribution of loading and temperature rise to demagnetization, since the demagnetization happens due to a loading and the temperature rise together.

The demagnetization is defined in this paper as a relative drop of open-circuit EMF.

#### A. Single Run Versus Iterating

The easiest way to study the demagnetization of the machine is to model the demagnetizing situation when the rotor is rotating at the constant synchronous speed. This kind of modeling does not take into account the change of the power angle, i.e., the angle between the rotor magnetization and the stator field, due to the demagnetization.

A demagnetization of the machine loaded with a constant torque should be modeled with an iterative process, where after each calculation with a constant rotor speed leading to demagnetization, the power angle is adjusted to give the same torque. After the adjustment, the calculation is repeated.

The purpose of the first test is to find out, how much difference there will be in the calculation results of a single run and the iterative modeling. It is also important to notice, if the demagnetization stops at a certain level, or if it drifts forward until the machine stalls.

#### B. Moment of Inertia

The demagnetization of a machine loaded with a constant torque can be accurately defined using a mechanical model, where the rotor speed is a function of the torque generated by the machine, and where the moment of inertia of the rotor is known. With the mechanical model, the rotor rotates in synchronization with the sinusoidal stator field, but the power angle can change according to the loading.

When this model is used, the demagnetization will lead to a decaying oscillation of the power angle, in which the time constant of the oscillation is many times longer than the cycle time of the input voltage. This will cause a very long simulation time.

The purpose of this second test was to find out, if the moment of inertia has significance on the results, and to verify the accuracy of the first test with iterative approach. The second test was simulated using four different moments of inertia for the rotor: the real value, a value ten times the real value, a value a hundred times the real value, and a value of one tenth of the real value. The rated supply frequency was used in all cases.

#### C. Squareness of the Hysteresis Curve

Magnet material of good quality has a hysteresis curve with a good squareness. The squareness is good, if the curve of magnetic polarization as a function of the applied field forms a tight angle in the second quadrant.

The purpose of this test is to model the effect of the curve squareness on the results of the demagnetization calculations. Two materials with different curve squarenesses are modeled. The high temperature curves of the materials are presented in Fig. 5.

#### D. Heating by Demagnetization

The third test takes into account the rise of temperature caused by the demagnetization like described in Fig. 1. This simulation is done stepwise. First, the losses and the temperatures are defined with the help of the thermal model but without using the demagnetization model. Then the demagnetization in that temperature is calculated. After that, the losses and temperatures are calculated again. This is repeated time after time, until the demagnetization stabilizes or the machine stalls. The purpose of this test is to see, if the demagnetization process

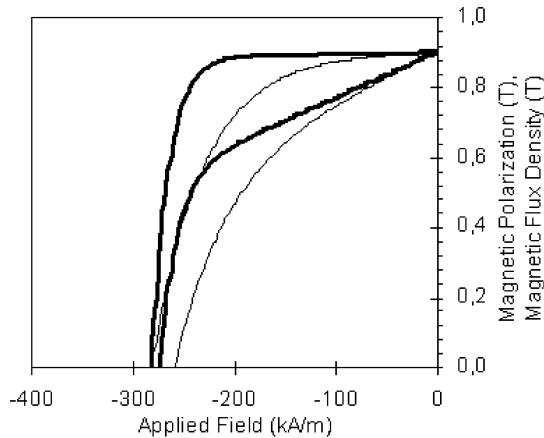


Fig. 5. The second quadrant hysteresis curves of the modeled sintered NdFeB magnets in 190°C. The thick curves are for the material with good squareness. The thin curves are for the material with bad squareness. The demagnetization model uses the shape of these curves as described in [5] and [9].

TABLE II  
RESULTS OF THE DEMAGNETIZATION CALCULATIONS AFTER EACH  
CALCULATION STEP

Modeling Situation	Demagnetization / Load Angle (Curve with good squareness) $T_{rotor} = 190^{\circ}\text{C}$ , $T_{stator} = 180^{\circ}\text{C}$	Demagnetization / Load Angle (Curve with bad squareness) $T_{rotor} = 190^{\circ}\text{C}$ , $T_{stator} = 180^{\circ}\text{C}$	Demagnetization / Load Angle (Curve with bad squareness) $T_{rotor} = 180^{\circ}\text{C}$ , $T_{stator} = 170^{\circ}\text{C}$
Single run	<b>-4.1 % / 35.6°</b>	<b>-15.9 % / 35.9°</b>	<b>-4.5 % / 35.2°</b>
Iterated			
Step 1	<b>-4.1 % / 35.6°</b>	<b>-15.9 % / 35.9°</b>	<b>-4.5 % / 35.2°</b>
Step 2	-4.5 % / 38.4°	-18.4 % / 47.3°	-4.7 % / 37.4°
Step 3	-4.6 % / 38.6°	-18.9 % / 49.1°	<b>-4.7 % / 37.6°</b>
Step 4	<b>-4.6 % / 38.6°</b>	-19.0 % / 49.7°	
Step 5		-19.1 % / 49.8°	
Step 6		<b>-19.1 % / 49.9°</b>	

stops at a certain level or if it drifts forward until the machine stalls.

## V. RESULTS AND DISCUSSION

In the first test, the machine was modeled for two electric cycles while the rotor was rotating at the constant speed. After the demagnetization simulation, the power angle was adjusted so, that the machine gave the torque required. Then the simulation was continued for two more electric cycles. The modeling was done for magnets with the two different hysteresis curve squarenesses. The case with the worse curve squareness was modeled at two temperatures. The results of the first test are presented in Table II.

The second tests were done including the mechanical model, where the rotor speed was dependent on the torque allowing the change of the power angle during the simulation. The loading torque was constant. The length of the test was 400 electric cycles. The results were also checked after 200 cycles. The demagnetization did not change between the 200 and 400 cycles. The calculation was repeated four times using the different moments of inertia, respectively. The results are presented in Table III. The results in Table III correspond to the first case presented in Table II. It can be assumed that the results in Table III are the

TABLE III  
RESULTS OF THE DEMAGNETIZATION CALCULATIONS WITH DIFFERENT  
MOMENTS OF INERTIA

Modeling Situation	Demagnetization (Curve with good squareness) $T_{rotor} = 190^{\circ}\text{C}$ , $T_{stator} = 180^{\circ}\text{C}$
Single run	-4.12 %
Iterated	-4.56 %
$I = I_{norm} / 10$	-4.61 %
$I = I_{norm}$	-4.61 %
$I = I_{norm} \times 10$	-4.56 %
$I = I_{norm} \times 100$	-4.56 %

$I_{norm}$  denotes the moment of inertia of the rotor,  $T_{rotor}$  and  $T_{stator}$  denote the temperatures of the rotor and the stator respectively.

TABLE IV  
RESULTS OF THE DEMAGNETIZATION CALCULATIONS WITH THERMAL MODEL

Test / Step	$T_{stator}$ (°C)	$T_{rotor}$ (°C)	Demagnetization	$P_{Cu}$ (W)	$P_{Total}$ (W)
Test 1 / S 0	180	190	0 %	911	3095
Test 1 / S 1	180	190	-4.6 %	1517	3768
Test 1 / S 2	194	200	-44.7 %	---	---
			STALL		
Test 2 / S 0	175	185	0 %	881	3064
Test 2 / S 1	175	185	-0.84 %	901	3085
Test 2 / S 2	176	186	-1.12 %	906	3089
Test 2 / S 3	176	186	-1.12 %	911	3095

most accurate ones, because the model used in that test is physically the most accurate one.

The results in Table II show that if the demagnetization is tested with a single run only, the result will be slightly too optimistic. However, after several iterations, the demagnetization reaches the same values as presented in Table III. Thus, it makes sense to make several iterations when predicting demagnetization instead of making a single long run. It is also interesting to notice that the demagnetization stabilizes to a certain level even with the material having the bad curve squareness, if the thermal effects are ignored.

In the last test, the same situation that was used to achieve the results presented in the first case of Table II was repeated including the results from the thermal model. The test led to stalling of the machine. Then, the test was repeated at a slightly smaller ambient temperature. In this case, the demagnetization was stabilized after some iteration. The results of the last test are presented in Table IV.

It is interesting to notice that the modeling without the thermal model (the first case in Tables II and III) led to a stable situation, while the modeling of the same situation with the thermal model leads to stalling (The first case in Table IV). In a real situation, the stalling would have happened after a while, because it will take some time before the final rotor temperature is reached.

When an overheated electric motor loaded with a constant torque demagnetizes, the motor starts to draw more current to keep the torque. This can be seen in Table II as an increase of the load angle. The increased current will cause more copper losses and thus, increased machine temperatures, as can be seen

in Table IV. The properties of a permanent magnet material and the resistivity of the windings are highly temperature dependent. The increase of temperature will cause a decrease of the intrinsic coercivity of the permanent magnet material, which will again cause demagnetization. This cycle can easily go on and on until the machine stalls. The last test clearly shows that a thermal model must be included in demagnetization calculations to get reliable results.

According to the simulations here, only a very small demagnetization led to a stable operation. The result is of course highly dependent on the thermal behavior of the machine. In most small or middle power motors, the thermal connection between the rotor and stator is quite strong, and the increase in stator winding temperature will lead to an increase in the rotor temperature, which will cause more demagnetization and will eventually lead to stalling.

## VI. CONCLUSION

The dynamics of the demagnetization of a permanent magnet machine was discussed. A demagnetization model, a thermal model and a special dovetail motor were presented. The demagnetization was modeled in several situations. It was noted that a thermal model of the machine must be used for accurate demagnetization modeling, because the demagnetization will cause an increase of the machine temperatures.

## ACKNOWLEDGMENT

This work was supported by Finnish Cultural Foundation, Research Foundation of Helsinki University of Technology, Ulla Tuomisen Säätiö and High Technology Foundation of Satakunta.

## REFERENCES

- [1] G.-H. Kang, J. Hur, H. Nam, J.-P. Hong, and G.-T. Kin, "Analysis of irreversible magnet demagnetization in line-start motors based on the finite-element method," *IEEE Trans. Magn.*, vol. 39, no. 3, pp. 1488–1491, May 2003.
- [2] G.-H. Kang, J. Hur, H.-G. Sung, and J.-P. Hong, "Optimal design of spoke type BLDC motor considering irreversible demagnetization of permanent magnet," in *Sixth Int. Conf. Electrical Machines and Systems, ICEMS 2003*, vol. 1, pp. 234–237.
- [3] M. Rosu, J. Saitz, and A. Arkkio, "Hysteresis model for finite-element analysis of permanent-magnet demagnetization in a large synchronous motor under a fault condition," *IEEE Trans. Magn.*, vol. 41, no. 6, pp. 2118–2123, Jun. 2005.
- [4] J. H. Lee and J. P. Hong, "Permanent magnet demagnetization characteristic analysis of a variable flux memory motor using coupled Preisach modeling and FEM," *IEEE Trans. Magn.*, vol. 44, no. 6, pp. 1550–1553, Jun. 2008.
- [5] S. Ruoho, E. Dlala, and A. Arkkio, "Comparison of demagnetization models for finite-element analysis of permanent magnet synchronous machines," *IEEE Trans. Magn.*, vol. 43, no. 11, pp. 3964–3968, Nov. 2007.
- [6] J. Farooq, S. Srairi, A. Djerdir, and A. Miraoui, "Use of permeance network method in the demagnetization phenomenon modeling in a permanent magnet motor," *IEEE Trans. Magn.*, vol. 42, no. 4, pp. 1295–1298, Apr. 2006.
- [7] K.-C. Kim, S.-B. Lim, D.-H. Koo, and J. Lee, "The shape design of permanent magnet for permanent magnet synchronous motor considering partial demagnetization," *IEEE Trans. Magn.*, vol. 42, no. 10, pp. 3485–3487, Oct. 2006.
- [8] B.-K. Lee, G.-H. Kang, J. Hur, and D.-W. You, "Design of spoke type BLDC motors with high power density for traction applications," in *IEEE Ind. Appl. Conf.*, 2004, vol. 2, pp. 1068–1074.

- [9] S. Ruoho and A. Arkkio, "Partial demagnetization of permanent magnets in electrical machines caused by an inclined field," *IEEE Trans. Magn.*, vol. 44, no. 7, pp. 1773–1778, Jul. 2008.
- [10] K.-C. Kim, K. Kim, H. J. Kim, and J. Lee, "Demagnetization analysis of permanent magnets according to rotor types of interior permanent magnet synchronous motor," *IEEE Trans. Magn.*, vol. 45, no. 6, pp. 2799–2802, Jun. 2009.
- [11] S. Ruoho and A. Arkkio, "Mixed-grade pole design for permanent magnet synchronous machines," presented at the ACEMP'07 and ELECTROMOTION'07 Joint Meeting, Bodrum, Turkey, Sep. 10–12, 2007.
- [12] S. Ruoho, J. Kolehmainen, J. Ikäheimo, and A. Arkkio, "Demagnetization testing for a mixed-grade dove-tail permanent magnet machine," *IEEE Trans. Magn.*, accepted for publication.
- [13] J. Rosero, J. Cusido, A. Garcia, J. Ortega, and L. Romeral, "Study on the permanent magnet demagnetization fault in permanent magnet synchronous machines," in *IEEE 32nd Annu. Conf. Industrial Electronics, IECON 2006*, Nov. 6–10, 2006, pp. 879–884, ISBN: 1-4244-0390-1.
- [14] J. Kolehmainen, "Rotor for a Permanent-Magnet Electrical Machine," WO Patent 2008025873 (A1), Mar. 6, 2008.
- [15] J. Kolehmainen, "Machine with a rotor structure supported only by buried magnets," in *Int. Symp. Electromagnetic Fields*, Prague, Sep. 2007.
- [16] J. Kolehmainen, "Dovetail permanent magnet rotor solutions with different pole numbers," in *Proc. 2008 Int. Conf. Electrical Machines*, Paper ID 939.
- [17] J. Kolehmainen, "Optimal dovetail permanent magnet rotor solutions with various pole numbers," *IEEE Trans. Ind. Electron.*, accepted for publication.
- [18] J. Kolehmainen and J. Ikäheimo, "Motors with buried magnets for medium-speed applications," *IEEE Trans. Energy Convers.*, vol. 23, no. 1, pp. 86–91, Mar. 2008.
- [19] A. Arkkio, "Analysis of Induction Motors Based on the Numerical Solution of the Magnetic Field and Circuit Equations," Ph.D. thesis, Acta Polytechnica Scandinavica, Helsinki, 1987, no. 59.
- [20] J. Wang, W. Wang, K. Atallah, and D. Howe, "Demagnetization assessment for three-phase tubular brushless permanent-magnet machines," *IEEE Trans. Magn.*, vol. 44, no. 9, pp. 2195–2203, Sep. 2008.
- [21] M. Katter, "Angular dependence of the demagnetization stability of sintered Nd-Fe-B magnets," *IEEE Trans. Magn.*, vol. 41, no. 10, pp. 3853–3855, Oct. 2005.

**Sami Ruoho** was born in Pori, Finland, in 1973. He received the M.Sc. degree in applied physics from the University of Turku, Finland, in 1997. He is now pursuing the Ph.D. degree in the Department of Electrical Engineering, Helsinki University of Technology (TKK). His subject is the modeling of demagnetization of permanent magnets in permanent magnet machines.

Since 2002 he has been working for Neorem Magnets Oy, Ulvila, Finland.

**Jere Kolehmainen** (M'09) was born in Kuopio, Finland, in 1972. He received the M.Sc. and Ph.D. degrees in theoretical physics from the University of Jyväskylä, Jyväskylä, Finland, in 1996 and 2000, respectively.

Currently, he is working at ABB Oy, Motors, Vaasa, Finland. His current research interests include synchronous and induction AC machines and electromagnetic modeling.

**Jouni Ikäheimo** was born in Seinäjoki, Finland, in 1968. He received the M.Sc. and Ph.D. degrees in physics from Helsinki University of Technology, Espoo, Finland, in 1992 and 1996, respectively.

He is currently a R&D manager with ABB Oy, Motors, Vaasa, Finland.

**Antero Arkkio** was born in Vehkalahti, Finland, in 1955. He received the M.Sc. (Tech.) and D.Sc. (Tech.) degrees from Helsinki University of Technology, Finland, in 1980 and 1988, respectively.

He has been a Professor of electrical engineering (Electromechanics) at Helsinki University of Technology (TKK) since 2001. Before his appointment as a Professor, he was a Senior Research Scientist and Laboratory Manager at TKK. He has worked with various research projects dealing with modeling, design, and measurement of electrical machines.